

See discussions, stats, and author profiles for this publication at: <https://www.researchgate.net/publication/244461989>

# Electrical Switching in $\pi$ -Resonant 1D Intermolecular Channels

ARTICLE *in* NANO LETTERS · AUGUST 2002

Impact Factor: 13.59 · DOI: 10.1021/nl025599a

---

CITATIONS

44

---

READS

19

## 3 AUTHORS:



**Alain Rochefort**

Polytechnique Montréal

88 PUBLICATIONS 1,941 CITATIONS

SEE PROFILE



**Richard Martel**

Université de Montréal

162 PUBLICATIONS 12,134 CITATIONS

SEE PROFILE



**Phaedon Avouris**

IBM, T. J. Watson Research Center

519 PUBLICATIONS 45,754 CITATIONS

SEE PROFILE

# Electrical Switching in $\pi$ -Resonant 1D Intermolecular Channels

Alain Rochefort,<sup>\*,†</sup> Richard Martel,<sup>‡</sup> and Phaedon Avouris<sup>‡</sup>

*Groupe Nanostructures, Centre de recherche en calcul appliqué (CERCA), Montréal, (Qué) Canada H3X 2H9, Département de génie physique, École Polytechnique de Montréal, Montréal, (Qué) Canada H3C 3A7, and T. J. Watson Research Center, IBM Research Division, Yorktown Heights, New York 10598*

*Received April 30, 2002; Revised Manuscript Received May 30, 2002*

## ABSTRACT

We studied the influence of  $\pi$ -orbital coupling in a 1D stack of 4,4'-biphenyldithiol (BDT) on the resulting electronic and electrical properties of the assembly. The conduction and the field-switching properties of the BDT assembly are compared as the intermolecular distances are reduced to below 4 Å. The system in the regime of strong  $\pi$ -interactions shows large conductance modulations upon application of a transverse gate field. The switching mechanism involves a delocalized  $\pi$ -resonance, i.e., resonant tunneling in the intermolecular  $\pi$ - and  $\pi^*$ -bands of the BDT assembly. The transmission is found to be significantly higher in the  $\pi^*$ -resonance. This behavior is discussed in terms of the density of states distribution in the conducting states.

A key question in organic electronics involves the control of the  $\pi$ -electron overlap in conjugated molecules that is responsible for electrical conduction. Understanding and controlling these interactions is crucial for the development of high performance organic transistors<sup>1</sup> and other molecular devices.<sup>2</sup> In these devices, the  $\pi$ -overlap is typically weak which, along with existence of defects such as domain boundaries, leads to organic transistors with a low carrier mobility, usually less than 1 cm<sup>2</sup>/Vs. The hope is that by exploiting different packing configurations of the molecules produced by supramolecular self-organization, the  $\pi$ -overlap can be sufficiently increased to move transport from the slow polaronic to the fast band-transport limit.<sup>3</sup>

It is well known that intermolecular  $\pi$ -overlap interactions can vary substantially in molecular assemblies with different packing densities and possibly different molecular conformations. An example is provided by biphenyl (BP). In the gas phase, it has a twisted ground state, while crystalline biphenyl is quasi-planar.<sup>4</sup> In the crystal, biphenyl has a herringbone packing structure and a narrow  $\pi$ -band is formed.<sup>5</sup> However, the  $\pi$ -interactions are still weak and the conduction involves hopping. The  $\pi$ -overlap can be increased somewhat by imposing pressure on the crystal.<sup>6</sup> Another way to increase the intermolecular  $\pi$ -interaction is by placing appropriate substituents on the molecules that form intermolecular bonds squeezing the molecules together. A recent example is provided by molecular wires based on substituted benzene rings stacked rigidly together by hydrogen bonding.<sup>7</sup> Yet

another self-organization scheme that may prove to be a very powerful tool for controlling intermolecular interactions involves the formation of self-assembled molecular (SAM) layers on metal surfaces. Recently, transistors based on SAMs of arenes on gold were fabricated in both planar<sup>8</sup> and vertical<sup>9</sup> geometries. Arenethiol-SAM on gold usually forms incommensurate hexagonal structures closely packed together with the molecules aligned normal to the surface.<sup>10</sup> In these films, STM studies have shown evidence of weak lateral conduction, thereby indicating that some  $\pi$ -overlap is introduced by the packing or by the interactions with the gold surface.<sup>11</sup>

Here we present the results of tight-binding calculations on the transport characteristics of a model molecular system as a function of the strength of the intermolecular  $\pi$ -interaction and that of an external electric field. The model involves biphenyldithiol (BDT) molecules stacked in an ordered 1D structure. Our aim is to explore the transport behavior in this type of structure when the intermolecular  $\pi$ -interactions are strong enough so that band conduction or resonant tunneling can take place.

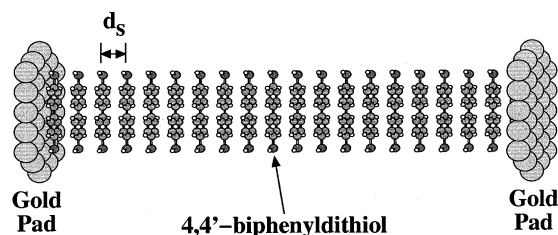
The electrical transport properties of 1D structures were computed using a Green's function approach<sup>12</sup> within the Landauer–Büttiker formalism. The Hamiltonian and overlap matrices used in this formalism were determined using the extended Hückel (EH) model that explicitly evaluates overlap matrix elements.<sup>13</sup> The electronic structure calculations were also performed within the EH formalism. The calculations were performed on 1D stacks<sup>14</sup> of 4,4'-biphenyldithiol molecules as a function of the intermolecular

\* Corresponding author.

<sup>†</sup> CERCA and École Polytechnique de Montréal.

<sup>‡</sup> IBM Research Division.

**Scheme 1.** Molecular Model of a Self-Assembled Monolayer (SAM) Made of 4,4'-Biphenyldithiol (BDT) Molecules (Separated by  $d_s$ ) Limited by Gold (111) Electrodes (29 Au Atoms)



distance ( $d_s$ ). The transport properties were evaluated in the stacking direction by placing gold electrode composed of 29 Au atoms with (111) crystal arrangement at both ends of the stack ( $d(\text{pad-BDT}) = 2.0 \text{ \AA}$ ) as shown in Scheme 1. To simulate the response of the system to a gate electric field, we used the approach discussed in a previous study.<sup>15</sup>

Figure 1 shows the variation of the density of states (DOS) of a SAM made of 20 BDT molecules stacked at intermolecular distances ranging from  $d_s = 3.0 \text{ \AA}$  to  $5.0 \text{ \AA}$ . As the intermolecular distance decreases, the  $\pi$ - and  $\pi^*$ -bands broaden due to the increased  $\pi$ - $\pi$  interaction between the BDT phenyl rings. At the shortest distance,  $d_s = 3.0 \text{ \AA}$ , the  $\pi$ - and  $\pi^*$ -bands are very broad and there is no apparent band gap. The number of BDT molecules in the SAM determines the value of the resulting band gap. The band gap is found to decrease sharply when the number of BDT molecules in the stack is increased from 1 to 10 BDT molecules (see inset), and then to converge to a stable value when about 20 molecules are stacked together.

The band structure calculations reported in Figure 2 for a 1D SAM of BDT are in line with our discussion of the band broadening. Additional information can also be extracted considering the dispersions of  $\pi^*$  ( $\approx +1 \text{ eV}$ ) and  $\pi$  ( $\approx -1.5 \text{ eV}$ ) levels as a function of  $d_s$ . At short distances (e.g.,  $3.0 \text{ \AA}$ ), the  $\pi$ - and  $\pi^*$ -bands cross the Fermi level at the  $\Gamma$  and  $K$  points, respectively. Therefore, stacking BDT molecules into a 1D SAM structure brings in new features at the  $\Gamma$  and  $K$  points in the vicinity of  $E_F$  that originate from the frontier orbitals (HOMO and LUMO) of the individual BDT molecules. More precisely, the interaction of the HOMO ( $\pi$ -orbital) and the LUMO ( $\pi^*$ -orbital) leads to 1D  $\pi$ -resonant states. These states are delocalized along the wire axis and form a 1D  $\pi$ -channel for electrical transport. Furthermore, the calculated electronic bandwidths of BDT-SAM with  $d_s$  up to  $4.0 \text{ \AA}$  are much larger than the phonon frequencies.

Details of the  $\pi$ -state interactions are shown in Figure 3. The HOMO and LUMO wave function contours of the 4,4'-biphenyldithiol in the stack of molecules are plotted for intermolecular distances of  $4.0 \text{ \AA}$  (Figure 3A) and  $3.3 \text{ \AA}$  (Figure 3B). We note that the wave functions involve  $\pi$ -(HOMO) and  $\pi^*$ -(LUMO) states that are antibonding and bonding relative to the stack, respectively. Thus, the bonding  $\pi$ -state of the individual molecule is antibonding with respect to the intermolecular bonding, and its wave function presents twice as many nodes compared to the 1D  $\pi^*$ -LUMO state. We can then understand why the HOMO and LUMO orbital

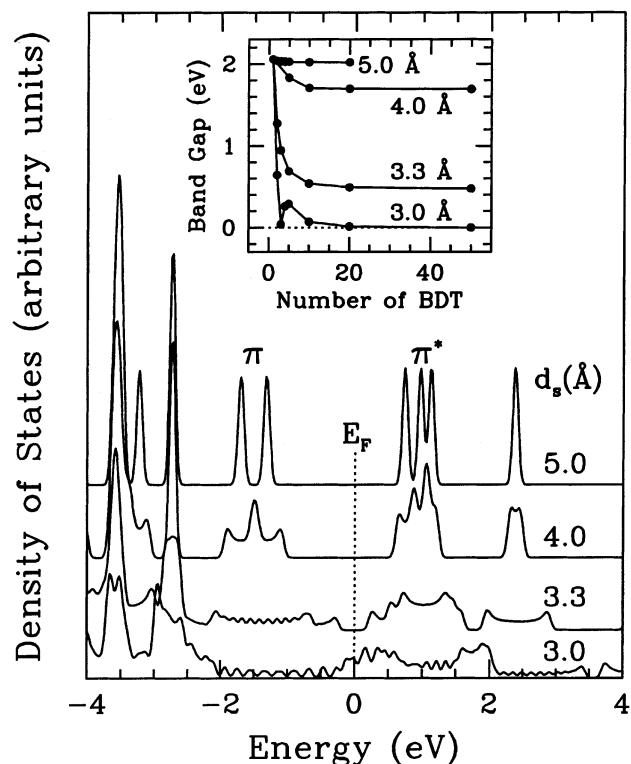


**Figure 1.** Variation of the density of states (DOS) of a stack of 20 BDT molecules as a function of the intermolecular distance  $d_s$ . The inset gives the change in the band gap of 4,4'-biphenyldithiol assembly as a function of the number of molecules in the SAM at  $d_s = 3.0, 3.3, 4.0$ , and  $5.0 \text{ \AA}$ .

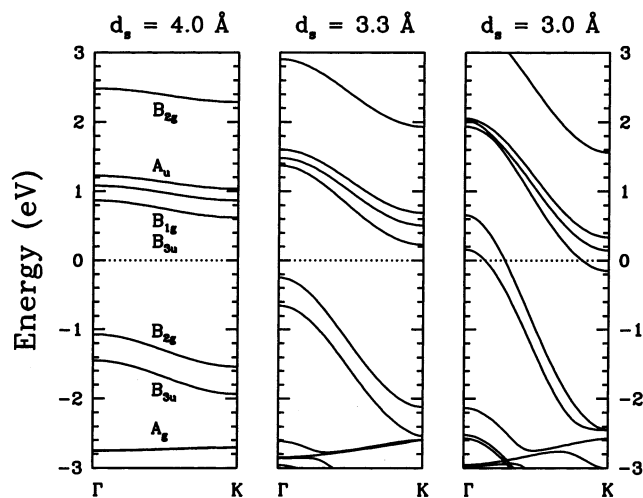


**Figure 2.** Band structure of the 1D SAM as a function of the intermolecular distance  $d_s$ . The calculated bandwidths are 0.4, 1.8, and  $3.2 \text{ eV}$  for  $\pi$ -HOMO (valence band), and 0.2, 1.0, and  $1.6 \text{ eV}$  for  $\pi^*$ -LUMO (conduction band), for  $d_s = 4.0, 3.3$ , and  $3.0 \text{ \AA}$ , respectively. The Fermi energy is indicated by the dotted line. The symmetry labels of bands following  $D_{2h}$  group are also given in the panel with  $d_s = 4.0 \text{ \AA}$ .

energies move in opposite directions at the  $\Gamma$  point as the distances between molecules are changed. This behavior is characteristic of this 1D system. Moreover, the band gap of the assembly depends on the strength of the HOMO and LUMO state interactions. In short, strong interactions lead

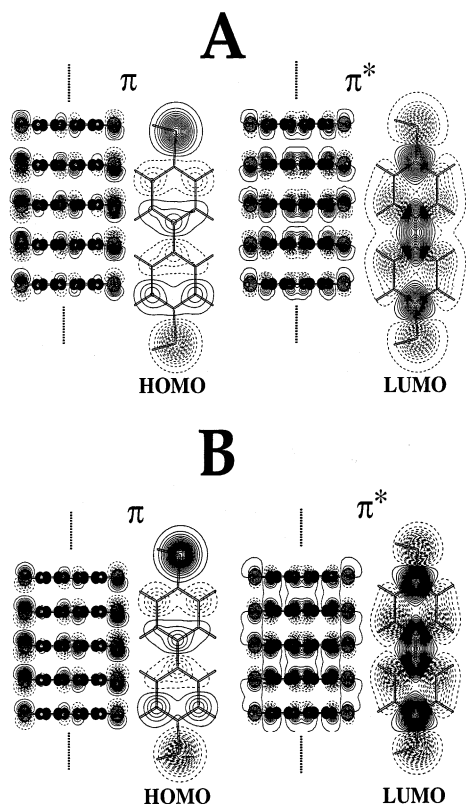


**Figure 3.** Wave function contours of frontier orbitals along the 1D direction and for individual BDT molecules for  $d_s = 4.0$  Å (upper panel, A) and  $3.3$  Å (lower panel, B). Each representation shows a side view (normal to the stacking direction) and a front view (in the stacking direction) of the BDT-SAM wave function contours.

to the formation of a smaller and indirect band gap, as shown in Figure 2.

We now concentrate on the electrical properties of the assembly in the stacking direction. Band transport is expected only in systems with significant dispersion of the  $\pi$ -states. In the case of BDT-SAM, this means that only distances of about the van der Waals size of a phenyl group ( $3.3$  Å  $\times$   $6.4$  Å) need to be considered (i.e.,  $d_s$  between  $3.0$  and  $4.0$  Å). Figure 4 shows the variation of the transmission function ( $\bar{T}(E)$ ) for  $d_s = 3.0, 3.3, 3.5$ , and  $4.0$  Å (lower four panels) and the logarithmic representation of some of these curves (upper panel) as a function of energy. The only noticeable changes in the transmission function at  $d_s = 4.0$  Å are observed in the upper panel where narrow modulations of the transmission are observed at about  $+1$  eV and  $-1.5$  eV. More important changes occur for a BDT-SAM with  $d_s = 3.3$ – $3.5$  Å. Large modulations of the transmission function (at least 8 orders of magnitude) are observed, associated with two strong transmission resonances centered at  $+1.0$  eV and between  $-1$  and  $-2$  eV. The lower panel ( $3.3$  Å) indicates that the transport, which is slightly more efficient in the conduction band (formed by the  $\pi^*$ -states), reaches a maximal value of about  $\bar{T}(E) = 2$ , and then decreases to zero at higher electron energies. This value is the maximum conductance for a doubly degenerate  $\pi$ -state. Finally, at  $d_s = 3.0$  Å, we observe a high transmission function ( $\bar{T}(E) > 2$ ) over a large range of energy but only a weak modulation of the

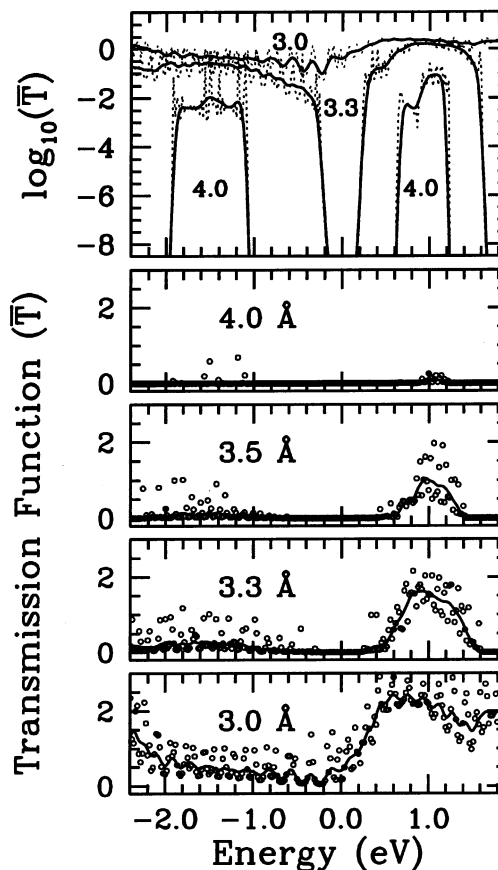


**Figure 4.** Influence of SAM stacking on the electrical properties of BDT in the 1D direction. The four lower panels show the variation of the transmission function ( $\bar{T}(E)$ ) for  $d_s = 3.0, 3.3, 3.5$ , and  $4.0$  Å while the upper panel gives a logarithmic representation of the calculated modulation of  $\bar{T}(E)$ .

conductance is possible. In this regime, the 1D molecular wire is metallic and other low-lying orbitals start contributing significantly to the transmission function. These results show that electrical transport in BDT-SAM occurs through the participation of  $\pi$ -resonant states that form a 1D channel. This conduction mechanism is only possible when the intermolecular interactions are strong ( $3.0 < d_s < 4.0$  Å).

One important property to evaluate is the response of the 1D channel transport to an external electric field (gate field). Figure 5 shows the 1D conductance ( $G$ ) at the Fermi energy ( $E_F$ ) as a function of the applied electric field<sup>16</sup> for two different intermolecular distances ( $3.3$  and  $4.0$  Å). The BDT-SAM with  $d_s = 3.3$  Å can switch effectively through a well defined  $\pi$ -resonance at a positive electric field, leading to a modulation of the conductance by more than 8 orders of magnitude, i.e., to a conductance value of  $2G_0 (= 4e^2/h)$ . The conductance is also affected by a negative gate field, but the  $\pi$ -resonance peak is much broader and less intense than that observed with a positive field. This difference in behavior can be understood on the basis of the bonding character of the conduction and valence bands. As shown in Figure 3(B), the LUMO at  $d_s = 3.3$  Å has a fully delocalized  $\pi$ -channel along the molecular stacking axis which indicates an effective channel for electric transport. This  $\pi^*$ -band (LUMO) contrasts with the band formed by the HOMO ( $\pi$ -

This article was released ASAP on 6/12/2002 with a typographical error in the final paragraph. The corrected version was posted on 6/18/2002.

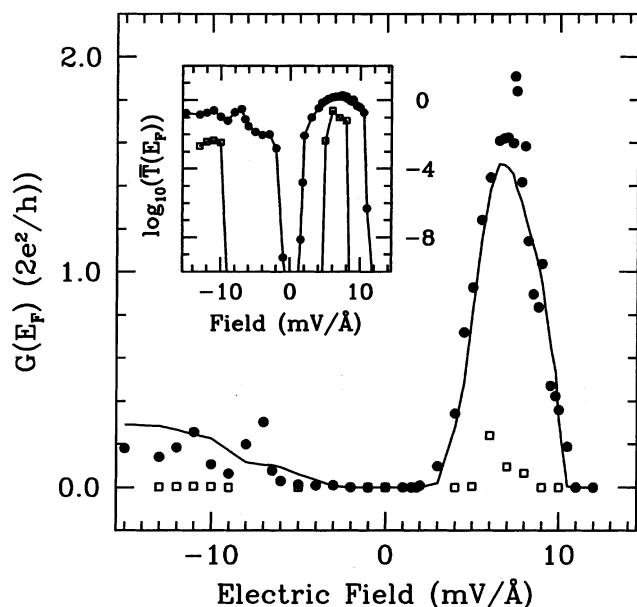


**Figure 5.** Modulation of the transmission function as a function of an external electrical field applied perpendicular to the SAM. The source of the external field is located at 100 Å from the SAM. The full circles represent the transmission function taken at  $E_F$  while the full curve represents an average of the signal at  $\pm 0.2$  eV from  $E_F$ . The inset shows the large ON/OFF ratio expected for BDT stacked at  $d_s = 3.3$  (full circles) and 4.0 Å (empty squares).

band), which has a wave function with most of its amplitude on the thiol groups rather than on the phenyl groups. The stronger participation of the thiol groups to the  $\pi$ -band (HOMO) compared to the phenyl moieties attenuates the transport in the valence band.

Finally, we need to compare the Au–SAM–Au configuration discussed above (end configuration) with the more conventional configuration where the SAM is sandwiched between gold electrodes through the thiol groups (top configuration). Although similar orbitals are involved in the transport in both side and top configurations, the transmission functions are significantly different. Preliminary results indicate that the top configuration for a SAM made of 20 interacting BDT molecules (i.e.,  $d_s \leq 5.0$  Å) has ON–OFF ratios that are several orders of magnitude lower compared to the end configuration presented here. The strengthening of the  $\pi$ -interactions increases the conductance in the OFF state of the top configuration, leading to a lower ON–OFF ratio.<sup>17</sup> Therefore, these results suggest that better transistor action is to be expected with the end configuration provided that the  $\pi$ -interactions are sufficiently strong.

**Acknowledgment.** A.R. thanks the Réseau québécois de calcul haute performance (RQCHP) for providing computational facilities.

## References

- (1) A special issue in IBM Journal of Research and Development with a review by C. D. Dimitrakopoulos and D. J. Masearo; *IBM J. Res. Develop.* **2001**, 45, 11.
- (2) (a) Joachim, C.; Gimzewski, J. K.; Aviram, A. *Nature* **2000**, 408, 541. (b) *Molecular Electronics: Science and Technology*; Aviram, A., Ratner, M. A., Eds.; New York Academy of Science: New York, 1998. (c) Reed, M. A. *Proc. IEEE* **1999**, 87, 652.
- (3) Sirringhaus, H.; Brown, P. J.; Friend, R. H.; Nielsen, M. M.; Bechgaard, K.; Langeveld-Voss, B. M. W.; Spiering, A. J. H.; Janssen, R. A. J.; Meijer, E. W.; Herwig, P.; de Leeuw, D. M. *Nature* **1999**, 401, 685.
- (4) See Hargreaves, A.; Hasan Rizvi, S. *Acta Crystallogr.* **1962**, 15, 365; a torsion of about 15° is also reported by Baudour, B. L. *Acta Crystallogr.* **1991**, B47, 935 but it is smeared out to average 0°.
- (5) See recent band structure calculation by Puschnig, P.; Ambrosch-Draxl, C. *Phys. Rev. B* **1999**, 60, 7891.
- (6) Puschnig, P.; Ambrosch-Draxl, C.; Heimel, G.; Zojer, E.; Resel, R.; Leising, G.; Kriechbaum, M.; Graupner, W. *Synth. Met.* **2001**, 116, 327.
- (7) Bushed, M. L.; Hwang, A.; Stephens, P. W.; Nuckolls, C. *J. Am. Chem. Soc.* **2001**, 123, 8157.
- (8) (a) Collet, J.; Tharaud, O.; Chapoton, A.; Vuillaume, D. *Appl. Phys. Lett.* **2000**, 76, 1941. (b) Collet, J.; Lenfant, S.; Vuillaume, D.; Bouloussa, O.; Rondelez, F.; Gay, J. M.; Kham, K.; Chevrot, C. *Appl. Phys. Lett.* **2000**, 76, 1339.
- (9) Schön, J. H.; Meng, H.; Bao, Z. *Nature* **2001**, 413, 713.
- (10) (a) Leung, T. Y. B.; Schwartz, P.; Scoles, G.; Schreiber, F.; Ulman, U. *Surf. Sci.* **2000**, 458, 34. (b) Yang, G.; Qian, Y.; Engtrakul, C.; Sita, L. R.; Liu, G.-Y. *J. Phys. Chem. B* **2000**, 104, 9059.
- (11) Ishida, T.; Mizutani, W.; Choi, N.; Akiba, U.; Fujihira, M.; Tokumoto, H. *J. Phys. Chem. B* **2000**, 104, 11680.
- (12) (a) Datta, S. In *Electronic Transport in Mesoscopic Systems*; Cambridge University Press: Cambridge, U.K., 1995. (b) Rochefort, A.; Avouris, Ph.; Lesage, F.; Salahub, D. R. *Phys. Rev. B* **1999**, 60, 13824.
- (13) Landrum, G. *YAEHMOP* (Yet Another Extended Hückel Molecular Orbital Package), Cornell University, Ithaca, NY, 1995.
- (14) The preferred arrangement of BDT–SAM layer on gold is not known. However, preliminary results obtained with scanning tunneling microscopy (STM) of the BDT–SAM on a Au(111) surface reveal the presence of disorder. These STM images show small domains of closely packed molecules standing both perpendicular and parallel to the surface. R. Martel et al., private communication.
- (15) Rochefort, A.; Di Ventra, M.; Avouris, Ph. *Appl. Phys. Lett.* **2001**, 78, 2521. The gate field is approximated as a capacitor field normal to the molecular stacking direction. In this case the external field ( $e\vec{E}e$ ) is a perturbation to the Hamiltonian where only diagonal terms are modified.
- (16) The external field is noncentrosymmetric with respect to the SAM axis (parallel to the gold leads), which is equivalent to a gate electrode located at around 100 Å from the SAM.
- (17) Rochefort, A.; Martel, R.; Avouris, Ph., to be published.

NL025599A